DAVID W. TAYLOR NAVAL SHIP
RESEARCH AND DEVELOPMENT CENTER
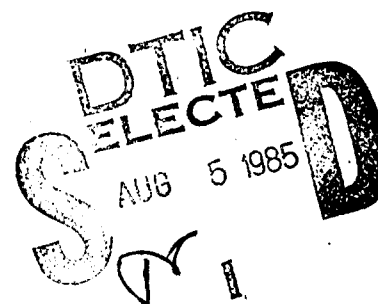
Bethesda, Maryland 20084

SWEEPS-STAGS FLUID ELEMENT GRID
REQUIREMENTS FOR ACCURATE REPRESENTATION OF
FLUID LOADING EFFECTS ON SUBMERGED VIBRATING STRUCTURES

by

Douglas E. Lesar
Rembert F. Jones, Jr.
David W. Taylor Naval Ship Research and Development Center
Bethesda, Maryland

APPROVED FOR PUBLIC RELEASE: DISTRIBUTION IS UNLIMITED
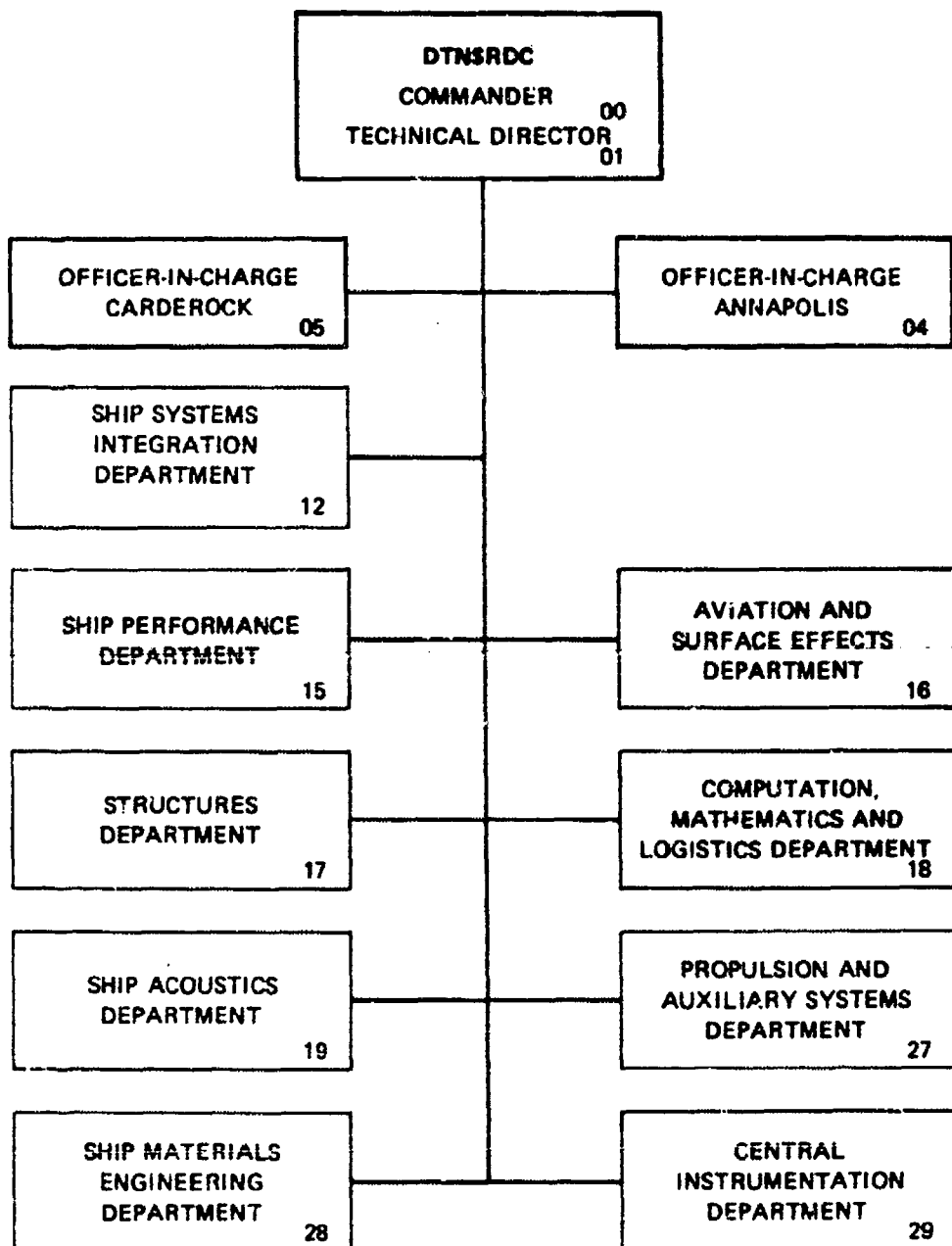
STRUCTURES DEPARTMENT

JUNE 1985   SD-85-43

MAJOR DTNSRDC ORGANIZATIONAL COMPONENTS

```
                    ┌──────────────────────────┐
                    │         DTNSRDC           │
                    │      COMMANDER      00    │
                    │  TECHNICAL DIRECTOR 01    │
                    └──────────────────────────┘
                                 │
        ┌────────────────────┐   │   ┌────────────────────┐
        │ OFFICER-IN-CHARGE  │───┼───│ OFFICER-IN-CHARGE  │
        │ CARDEROCK      05  │   │   │ ANNAPOLIS      04  │
        └────────────────────┘   │   └────────────────────┘
                                 │
        ┌────────────────────┐   │
        │  SHIP SYSTEMS      │   │
        │  INTEGRATION       │───┤
        │  DEPARTMENT    12  │   │
        └────────────────────┘   │
                                 │
        ┌────────────────────┐   │   ┌────────────────────┐
        │ SHIP PERFORMANCE   │   │   │  AVIATION AND      │
        │ DEPARTMENT     15  │───┼───│  SURFACE EFFECTS   │
        │                    │   │   │  DEPARTMENT    16  │
        └────────────────────┘   │   └────────────────────┘
                                 │
        ┌────────────────────┐   │   ┌────────────────────┐
        │ STRUCTURES         │   │   │ COMPUTATION,       │
        │ DEPARTMENT     17  │───┼───│ MATHEMATICS AND    │
        │                    │   │   │ LOGISTICS DEPT 18  │
        └────────────────────┘   │   └────────────────────┘
                                 │
        ┌────────────────────┐   │   ┌────────────────────┐
        │ SHIP ACOUSTICS     │   │   │ PROPULSION AND     │
        │ DEPARTMENT     19  │───┼───│ AUXILIARY SYSTEMS  │
        │                    │   │   │ DEPARTMENT     27  │
        └────────────────────┘   │   └────────────────────┘
                                 │
        ┌────────────────────┐   │   ┌────────────────────┐
        │ SHIP MATERIALS     │   │   │ CENTRAL            │
        │ ENGINEERING        │───┴───│ INSTRUMENTATION    │
        │ DEPARTMENT     28  │       │ DEPARTMENT     29  │
        └────────────────────┘       └────────────────────┘
```

SWEEPS-STAGS FLUID ELEMENT GRID

REQUIREMENTS FOR ACCURATE REPRESENTATION OF

FLUID LOADING EFFECTS ON SUBMERGED VIBRATING STRUCTURES

Douglas E. Lesar
Rembert F. Jones, Jr.
David W. Taylor Naval Ship Research and Development Center
Bethesda, Maryland

JUNE 1985

A-1

ADMINISTRATIVE INFORMATION

ABSTRACT

The second order Doubly Asymptotic Approximation (DAA2) method developed by Geers and Felippa [1] has been implemented in the SWEEPS-STAGS code [2] to provide a steady-state vibration analysis capability for submerged structures. This paper extends the previous work of DeRuntz, Geers, and Felippa [1,3] in determining the convergence behavior of DAA2-predicted wet surface variables that are relevant to steady-state submerged structural vibrations. The convergence rates of "fluid boundary eigenvalues" and convergence behaviors of modal acoustic impedance functions are calculated for increasingly dense fluid element grids on a spherical surface. Within mode-dependent frequency ranges in which DAA2 is valid, dense grids on the order of five elements per half-wave are needed for five percent accuracy in modal acoustic impedance. This is a consequence of the low order (constant source strength) interpolation used for establishing fluid variables. There are mode-dependent frequency ranges for which DAA2 acoustic impedance predictions are inaccurate, even for very dense fluid element grids. These results provide guidance for engineers developing SWEEPS-STAGS idealizations for vibration analysis of complex submerged structures.

NOMENCLATURE

(Overdots denote differentiation with respect to time, e.g., $\dot{p}$ is first time derivative of pressure)

a_n = nth-mode wet surface element area

$\underline{A}_f$ = wet surface element area matrix

c = fluid sound speed

(c) = superscript denoting curvature-augmented DAA2

C_s = structural damping matrix

$\underline{f}_s$ = mechanical input force vector

g = mode-derived DAA2 empirical curvature parameter

G = structure coordinate – fluid coordinate transformation matrix

I = total number of fluid elements in spherical surface mesh

j = $\sqrt{-1}$

k = acoustic wave number

$\underline{K}_s$ = structural stiffness matrix

m = order of asymmetric spherical surface harmonic

(m) = superscript denoting mode-derived DAA2

m_n = nth-mode wet surface fluid mass

$\underline{M}_f$ = wet surface fluid mass matrix

$\underline{M}_s$ = structural mass matrix

n = order of axisymmetric spherical surface harmonic

p = wet surface pressure

$\underline{p}$ = wet surface pressure vector associated with fluid boundary eigenmode

$\underline{p}_i$ = incident wave wet surface pressure vector

$\underline{p}_r$ = wet surface-radiated pressure vector

r = spherical surface radius

s = Laplace transform variable

u = wet surface normal velocity

$\underline{u}$ = wet surface normal velocity vector associated with fluid boundary eigenmode

$\underline{u}_i$ = incident wave wet surface normal velocity vector

$\underline{u}_n$ = nth-mode wet surface normal velocity

$\underline{u}_s$ = wet surface normal velocity vector

2

$\underline{x}$ = structural displacement vector

Z_n = nth-mode (specific) acoustic fluid impedance

$\underline{\kappa}$ = diagonal matrix of wet surface mean local curvatures

K_n = nth-mode wet surface mean curvature

$\underline{\lambda}$ = diagonal matrix of fluid boundary eigenvalues

λ_n = nth-mode fluid boundary eigenvalue

ϱ = fluid density

$\underline{\Omega}_f$ = wet surface fluid-frequency matrix

ω = radian frequency

ω_n = nth-mode wet surface fluid-frequency parameter

INTRODUCTION

The steady-state time-harmonic interaction between submerged elastic structures and exterior acoustic fluid is an important Naval structural mechanics and acoustics problem. The finite element method (FEM) is the only viable means of modeling the vibratory response of harmonically-excited, topographically complex structure composed of beams, plates, and shells. The FEM, as a means of approximating the mass, stiffness, and damping distributions of arbitrary structures, is described in many texts; [4] is a well-known example. Various numerical schemes are available for "exact" modeling of linear acoustic fluid in time-harmonic problems; two important approaches are fluid finite elements [5,6,7] and Helmholtz surface integral equations [8,9,10]. Both of these fluid models have been coupled to structural finite element codes [11-15] such that vibration and sound radiation problems of coupled fluid-structure dynamical systems can be analyzed. Fluid finite element and Helmholtz surface integral approaches are three-dimensional and two-dimensional numerical methods of discretizing the wave equation. These methods are capable of exactly representing fluid loading effects on the wet surface of a submerged vibrating structure. Convergence toward exact solutions with increasing wet surface grid density is possible as long as propagating acoustic waves in the fluid domain and fluid boundary pressure distributions are resolved (Also, in certain Helmholtz integral methods the problem of uniqueness of solution has to be dealt with).

An alternative approximate acoustic fluid model is the second-order Doubly Asymptotic Approximation (DAA2), originally developed for transient fluid-structure interaction [16], and recently extended to time-harmonic vibrations of submerged structures [1]. DAA2 has also been exercised in simple coupled vibration and sound radiation problems [17]. Mathematically, DAA2 is a second-order differential equation that approximates the exact relationship between fluid pressure and velocity on a two-dimensional boundary of a three-dimensional infinite fluid domain. The boundary equations are, effectively, dimensionally-reduced versions of three-dimensional fluid field equations. Numerical implementation of DAA2 follows a boundary element method (BEM, also discussed in [4]), since the spatial variations of fluid pressure and velocity on the boundary of an infinite exterior fluid (wet surface of a submerged structure) are interpolated by assumed functions local to elements of the surface. The frequency domain impedance (ratio of pressure to velocity) approximation is governed by the order of the DAA equation used.

A structural dynamics analyst usually invokes many approximations when devising idealizations of complicated structures. The inherent assumptions of the mathematics underlying an analysis computer code (e.g., structural FEM coupled with fluid BEM in the present case) comprise an approximation level to be accepted at the onset. The analyst must endeavor to minimize the influence of discretization errors on predicted response variables. More often than not, the analyst faces the task of predicting the response of a submerged structure for which no previous modeling experience exists. In such cases, information on the ability of the chosen numerical method to represent the response of simple structures demonstrating known behavior is useful guidance for developing valid idealizations of complicated structures.

Valid FEM/BEM idealizations of vibrating submerged structures are those which correctly resolve structural bending and membrane travelling waves and resonant standing waves poorly controlled by structural damping. Similarly, the acoustic impedance that exterior fluid presents to the structural wet surface must be resolved in the frequency domain and in space. Mathematical idealizations have hope of meeting these requirements if they possess (1): a sufficient number of structural elements per wavelength of important bending or membrane response patterns, and (2): a sufficient number of fluid boundary elements per wavelength in important wet surface stationary or travelling response patterns. The optimum wet surface FEM/BEM grid depends on the interpolation orders of structural and fluid elements relative to the response pattern complexity.

This paper presents benchmark problem results that should be useful to users of the SWEEPS-STAGS code [2,18], which utilizes coupled structural FEM and DAA2-based fluid BEM for prediction of the nonlinear transient or linear time-harmonic response of submerged shell structures. In particular, the ability of the SWEEPS-STAGS fluid boundary elements and the DAA2 approximation to resolve the modal acoustic impedance functions of a spherical surface exposed to an infinite extent of external acoustic fluid is examined.

A DAA2 MODEL FOR ACOUSTIC IMPEDANCE

The DAA2 equations defining an approximate relationship between pressure and velocity on the surface of a submerged vibrating structure have been reported elsewhere [2], they are time-harmonic specializations of the transient equations [16]. The coupling of structural stiffness, structural damping, structural mass, and complex-valued acoustic fluid impedance is apparent in the DAA2 frequency domain matrix equations (eqs. (1) and (2) of [2]):

$$\begin{bmatrix} \underline{E}_{ss} & \underline{E}_{sf} \\ \underline{E}_{fs} & \underline{E}_{ff} \end{bmatrix} \begin{Bmatrix} \underline{x} \\ \underline{p}_s \end{Bmatrix} = \begin{Bmatrix} \underline{g}_s \\ \underline{g}_f \end{Bmatrix} \quad (1)$$

where

$\underline{E}_{ss} = -\omega^2 \underline{M}_s + j\omega \underline{C}_s + \underline{K}_s$

$\underline{E}_{sf} = \underline{G}\underline{A}_f$

$\underline{E}_{fs} = \varrho c \, (j\omega^3 \underline{M}_f \underline{G}^T + \omega^2 \underline{\Omega}_f \underline{M}_f \underline{G}^T)$

$\underline{E}_{ff} = -\omega^2 \underline{M}_f + \varrho c \, (j\omega \underline{A}_f + \underline{\Omega}_f \underline{A}_f)$

$\underline{g}_s = \underline{f}_s - \underline{G}\underline{A}_f \underline{p}_i$

$\underline{g}_f = \varrho c \, (\omega^2 \underline{M}_f - j\omega \underline{\Omega}_f \underline{M}_f) \, \underline{u}_i$

An approximate model of the pressure and velocity relationship on a closed surface within an exterior fluid of infinite extent, shown in Figure 1, can be obtained by suppressing all structural matrices and specifying zero incident-wave pressure and velocity. Under these conditions, the scattered pressure can be interpreted as radiated pressure and equation (1) reduces to

$$[-\omega^2 \underline{M}_f + \varrho c \, (j\omega \underline{A}_f + \underline{\Omega}_f \underline{A}_f)] \, \underline{p}_r + [\varrho c \, (j\omega^3 \underline{M}_f \underline{G}^T + \omega^2 \underline{\Omega}_f \underline{M}_f \underline{G}^T)] \, \underline{x} = 0 \quad (2)$$

The following transformation converts "structural" displacement vector $\underline{x}$ to wet surface velocity vector $\underline{u}_s$

$$\underline{u}_s = -j\omega \underline{G}^T \underline{x} \quad (3)$$

If $\underline{u}_s$ is imagined as describing modal standing wave motions of the fluid "boundary" in the absence of external driving forces
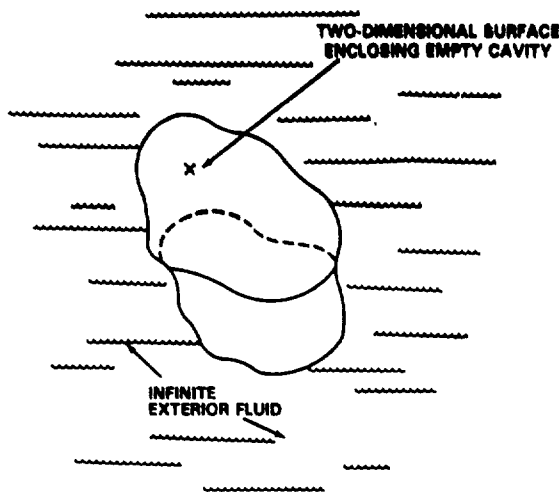
3

Figure 1 - Two-Dimensional Fluid Surface in Three-Dimensional Exterior Fluid Domain

f_s, then (2), when combined with (3), reduce to a frequency-domain relationship between fluid boundary pressures and velocities required to sustain these modes:

$$[-\omega^2 M_f + \varrho c \, (j\omega A_f + Q_f A_f)] \, p = [\varrho c (j\omega Q_f M_f - \omega^2 M_f)] \, u \tag{4}$$

An equivalent expression in the time domain is:

$$M_f \, \ddot{p} + \varrho c A_f \, \dot{p} + \varrho c Q_f A_f \, p = \varrho c \, (M_f \ddot{u} + Q_f M_f \, \dot{u}) \tag{5}$$

Equations (4) and (5) are the DAA2 equations defining the fluid pressure p on the surface of a fluid boundary vibrating freely with velocity distribution u at frequency ω. This interpretation of the conditions under which the general DAA2 fluid-structure expressions (1) were reduced to either (4) or (5) implies that DAA2 modal acoustic impedance functions can be defined for every fluid boundary "mode," provided the modes are uncoupled. This is possible only for a limited number of fluid surface geometries; the infinitely long cylindrical surface and the spherical surface are two examples. The spherical surface is considered here.

SPECIALIZATION TO SPHERICAL SURFACE

The acoustic impedance functions implied by the DAA2 differential equations relating wet surface pressure and velocity are derived for the two DAA2 forms (mode-derived $DAA_2^{(m)}$ and curvature-augmented $DAA_2^{(c)}$) in the Appendix. Equations (4) and (5) above are used as a basis for this development. When these two functions are specialized to uncoupled acoustic mode situations, the resulting complex-valued DAA2 acoustic impedance polynomials are functions of "fluid boundary mode" eigenvalues and radiated-wave curvature parameters. The notion of fluid boundary modes and the meanings of $DAA_2^{(m)}$ and $DAA_2^{(c)}$ are described more completely by Geers [16,19] and Felippa [20]. In $DAA_2^{(m)}$ the curvature parameter is a mode-independent empirical constant, while $DAA_2^{(c)}$ uses a matrix of local wet surface curvatures. As shown in the Appendix, the accuracy of DAA2-predicted wet surface modal acoustic impedance depends on the accuracy of computed fluid boundary eigenvalues. Fluid element grid densities needed for a given acceptable acoustic impedance error level in frequency ranges of DAA2 method validity can be readily defined for the spherical wet surface problem since the modal impedances are uncoupled. As shown in the Appendix, each DAA2-based complex

modal impedance is a function of one fluid boundary mode, each of which corresponds to the low frequency limit of the exact "accession to inertia per unit area" of an acoustic mode of a spherical surface.

The general expressions for $DAA_2^{(m)}$ and $DAA_2^{(c)}$ modal acoustic impedances, equations (A16) and (A17) of the Appendix, reduce to simpler forms when the normalizations $\varrho = c = r =$ unity are used for a spherical surface geometry. The $DAA_2^{(m)}$ empirical curvature parameter g is taken to be unity for the spherical surface, and the $DAA_2^{(c)}$ curvature function Q_n reduces to $1-\lambda_n$. With these particulars, equations (A16) and (A17) become:

$$DAA_2^{(m)} : \begin{cases} ReZ_n = \dfrac{(\omega \lambda_n)^4}{(\omega \lambda_n)^4 - (\omega \lambda_n)^2 + 1} \\[3mm] \dfrac{ImZ_n}{j\omega} = \dfrac{\lambda_n^4}{(\omega \lambda_n)^4 - (\omega \lambda_n)^2 + 1} \end{cases} \tag{6}$$

$$DAA_2^{(c)} : \begin{cases} ReZ_n = \dfrac{(\omega \lambda_n)^4}{(\omega \lambda_n)^4 - (\omega \lambda_n)^2 + g(\lambda_n)} \\[3mm] \dfrac{ImZ_n}{j\omega} = \dfrac{\lambda_n[g(\lambda_n) - \lambda_n(\omega \lambda_n)^2]}{(\omega \lambda_n)^4 - (\omega \lambda_n)^2 + g(\lambda_n)} \end{cases} \tag{7}$$

where $g(\lambda_n) = (\lambda_n^2 + 1) + 2\lambda_n((\omega \lambda_n)^2 - 1)$.

The "exact" low frequency limits of a spherical surface's fluid boundary eigenvalues, $\lambda_n = 1/(n+1)$, can be used in equations (6) and (7) to define "exact" DAA2 modal acoustic impedance functions Z_n. Approximate λ_n, as predicted for various SWEEPS-STAGS fluid element grids, can be substituted in the same expressions to obtain associated approximate Z_n. The convergence of Z_n and λ_n toward values based on exact fluid boundary eigenvalues (the best results possible with DAA2) with increasing fluid element grid density is now examined. Frequency ranges of DAA2 method validity are also determined by comparison to exact modal series solutions [21].

SWEEPS-STAGS MODAL IMPEDANCE RESOLUTION STUDY

Equations (6) and (7) show that DAA2 polynomial approximations of impedance functions Z_n depend only on frequency ω and fluid boundary eigenvalues λ_n. Thus, only the FLUMAS (Fluid Mass) module of the SWEEPS-STAGS code, which calculates fluid mass matrix M_f and solves the following fluid boundary eigenproblem, needed to be run in this study:

$$M_f u = \lambda A_f u \tag{8}$$

The fluid boundary eigenvalues and eigenvectors of a spherical surface of unit radius, immersed in a fictional acoustic fluid of unit density and sound speed, were determined for a series of uniform SWEEPS-STAGS fluid element meshes. The mesh family considered is shown in Figure 2; the four-noded fluid elements of the FLUMAS module of SWEEPS-STAGS were used in all cases.

As shown in DeRuntz and Geers [3], a three-dimensional spherical surface possesses repeating eigenvalues of many nonaxisymmetric wave number orders (m) for every value of axisymmetric wave number order (n) of n = 2 and above. Hence, FLUMAS produced as many repeated eigenvalues for n ≥ 2 as were allowed by the symmetry plane constraints specified in the quarter sphere idealizations of Figure 2. These eigenvalues occurred in the sequence (1 (n+1)), which is a reduction of equation 8.31 of Junger and Feit [22] for unit spherical surface radius and unit fluid density.

4

- ONLY GRID IN ONE SUBDIVISION SHOWN
- NUMBER OF ELEMENTS PERTAINS TO ENTIRE SPHERICAL SURFACE

FUNDAMENTAL SUBDIVISION

SYMMETRY PLANES

2x2

96 ELEMENTS

4x4

384 ELEMENTS

1x1
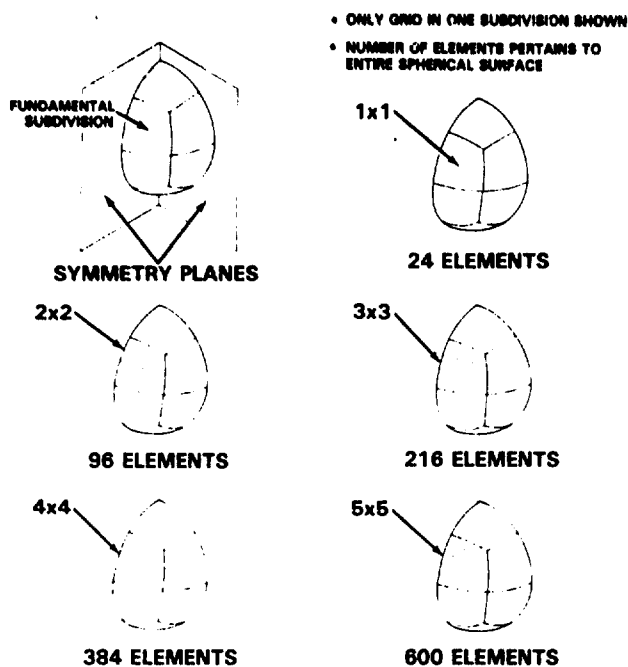
24 ELEMENTS

3x3

216 ELEMENTS

5x5
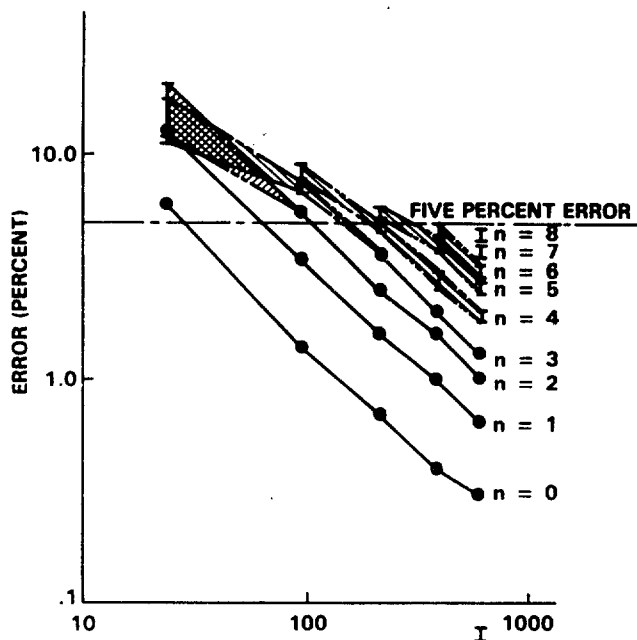
600 ELEMENTS

Figure 2 - Family of Fluid Element Meshes on a Spherical Surface

Figure 3 - Convergence of Spherical Surface Fluid Boundary Eigenvalues with Increasing Fluid Element Density

Figure 4 - Erroneous Mode-Derived DAA2 Prediction of Acoustic Impedance of N = 0 Mode

Figure 5a - Comparison of Sweeps-Stage Modal Acoustic Impedance Predictions to Exact Solution for Spherical Surface

In [3], convergence rates of fluid boundary eigenvalues were presented for n=0 and n=1 modes of a spherical surface. The present work extends these results to n ≥ 2. FLUMAS-computed fluid boundary eigenvalue convergence rates for the grids of Figure 2 are presented in Figure 3. These computations exhibit a convergence rate of roughly (1/I), where I is the number of elements in the mesh. These predictions agree, qualitatively, with those obtained earlier by DeRuntz and Geers [3]. The predicted differences between theoretically identical eigenvalues of like n-order but differing m-order become greater as n increases and/or grid density decreases. This is indicated by the error ranges drawn in Figure 3.
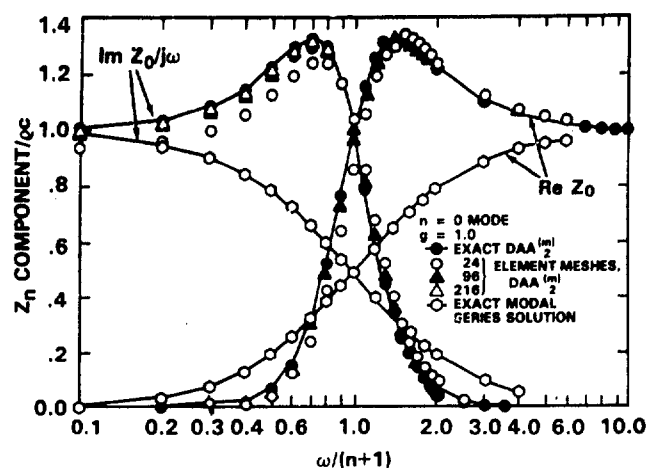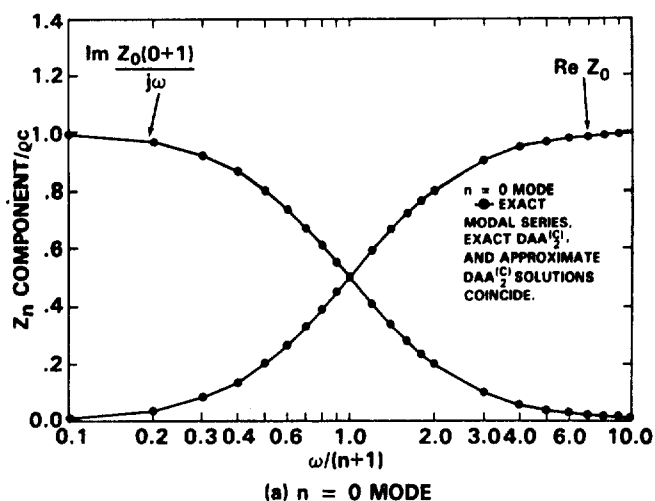
The DAA2 spherical surface impedance functions of equations (6) and (7) were calculated for each axisymmetric mode $0 \leqslant n \leqslant 4$, and for each mesh of Figure 2 in the normalized frequency range $0.1 < \omega/(n+1) < 10.0$. It is known that acoustic impedance follows a transition between high- and low-frequency asymptotic limits in this frequency range. The results of the impedance calculations are shown in Figures 4 and 5.

The mode-derived forms of DAA2 modal acoustic impedances given by equation (6) were found to be inadequate. Although convergence with increasing grid density occurred, the converged functions were totally erroneous. Figure 4 demonstrates this fundamental inadequacy of $DAA_2^{(m)}$ by comparison to exact fluid impedance functions of Felippa and Geers [21].

In certain frequency ranges, the $DAA_2^{(C)}$ polynomials of equations (7), with exact fluid boundary eigenvalues substituted, did not accurately represent the exact modal series acoustic impedance solutions [21]. This error reflects DAA2 frequency domain approximations and is independent of fluid element grid density. On the other hand, acoustic impedances based on approximate fluid boundary eigenvalues did converge to the exact modal series solution in frequency ranges where the exact DAA2 solutions are fair representations of exact modal series acoustic impedance.

The different convergence behaviors for n=0 through n=4 are illustrated in Figure 5. The modal series n=0 impedances are accurately predicted by $DAA_2^{(C)}$ in the entire frequency range $0.1 <$

Figure 5b - Comparison of Sweeps-Stags Modal Acoustic Impedance Predictions to Exact Solution for Spherical Surface (continued)

Figure 5d - Comparison of Sweeps-Stags Modal Acoustic Impedance Predictions to Exact Solution for Spherical Surface (continued)
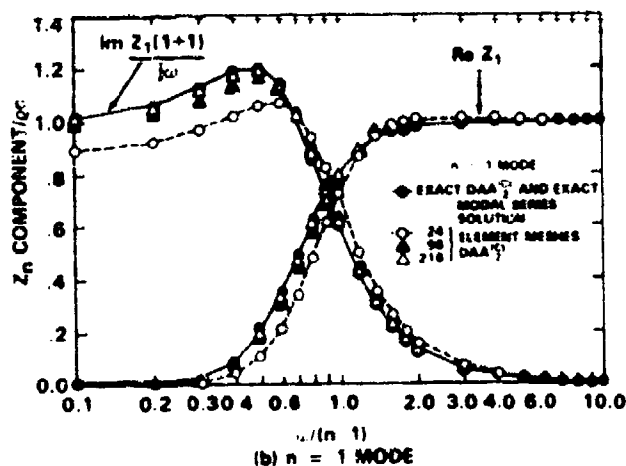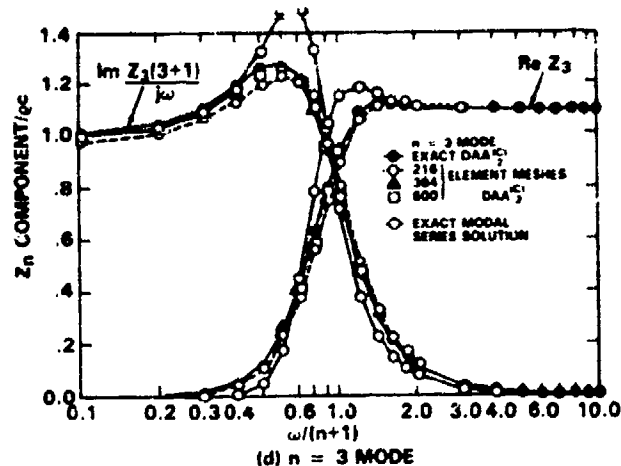

Figure 5c - Comparison of Sweeps Stags Modal Acoustic Impedence Predictions to Exact Solution for Spherical Surface (continued)

Figure 5e - Comparison of Sweeps-Stags Modal Acoustic Impedance Predictions to Exact Solution for Spherical Surface (continued)
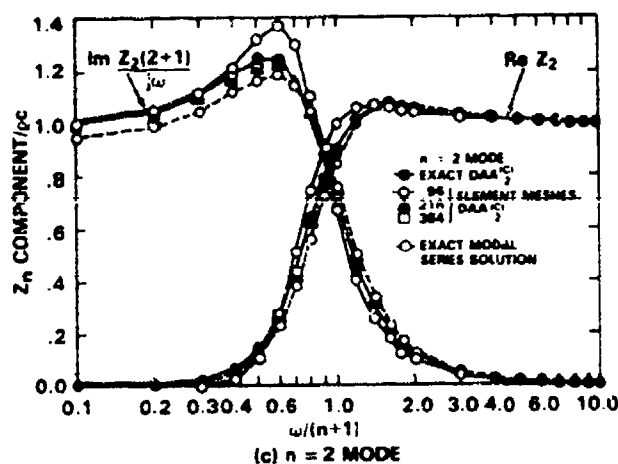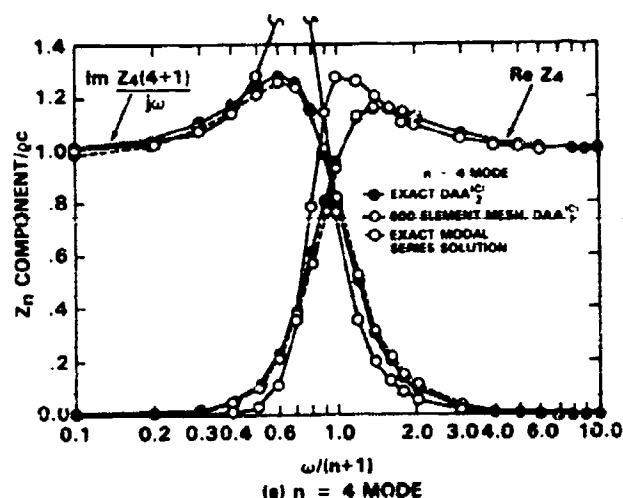
$\omega/(n+1) < 10.0$ even with a very coarse grid (Figure 5a). The DAA$_2^c$ $n=1$ impedances converged to the exact fluid boundary eigenvalue solution with increasing grid density. For $n=1$, the exact DAA$_2^{(c)}$ solutions are, like for $n=0$, essentially the exact modal series curves (Figure 5b). However, for $n=2$, 3 and 4, the exact DAA$_2^{(c)}$ solutions are not close to the modal series solutions in the entire frequency range of interest. Exact modal series, exact DAA$_2^c$ and approximate DAA$_2^{(c)}$ $n=2$ modal acoustic impedances are compared in Figure 5c for several fluid element grids. For $n=2$, the frequency domain errors dominate the acoustic reactance (Im Z_n) in the nondimensional frequency range $0.4 < \omega/(n+1) < 4.0$, and dominate the acoustic resistance (Re Z_n) for $\omega < 1.4$. This means that DAA2 is inherently incapable of properly representing the "added mass" effect in $n=2$ vibrations of a spherical surface, as governed by Im Z_n, in the dimensional frequency range $1.2 < \omega < 12.0$, and also will not accurately simulate radiation damping for $\omega < 4.2$. Figures 5d and 5e show similar

limiting ranges for $n=3$ and 4. The frequency ranges of validity for DAA$_2^{(c)}$ prediction of $n=2$, 3, and 4 modal acoustic impedances are summarized in Table 1.

The next consideration is the reduction of spatial discretization error in the applicability ranges listed in Table 1. The predicted magnitudes of impedance terms for the several grids considered here are compared to modal series and exact DAA$_2^{(c)}$ solutions in Tables 2 and 3. Another limiting factor illustrated in these tables is the inability of coarser fluid element grids to resolve fluid boundary eigenvalues and recognizable eigenvectors. The ratios of predicted to exact DAA2 fluid boundary eigenvalues (low frequency asymptotic values of accession to inertia per unit area) are given for various grid densities in Table 4. FLUMAS did predict multiple eigenvalues for the nonaxisymmetric modal patterns allowed by the two symmetry planes in the quarter-sphere wet surface idealizations. In a similar calculation by DeRuntz [18], a 384 element grid was unable to predict multiple eigenvalues for the nonaxisymmetric $m=11$ modal order. For this waveform the erroneous differences between predicted degenerate eigenvalues

6

TABLE 1 · FREQUENCY RANGES OF VALIDITY FOR CURVATURE—AUGMENTED DAA2

RATIOS OF Z_n COMPONENTS: (EXACT DAA$_2^{(C)}$/EXACT MODAL SERIES)

$\frac{\omega}{n+1}$	Im $Z_n (n+1)/\omega$					Re Z_n				
	n=0	n=1	n=2	n=3	n=4	n=0	n=1	n=2	n=3	n=4
0.1	1.000	1.000	1.004	1.005	1.005	1.000	1.000	2.00		
0.2			1.012	1.017	1.018			5.61		
0.3			1.007	1.023	1.031			3.16		
0.4			0.980	1.004	1.023			1.91		
0.5			0.934	0.943	0.970			1.33	2.50	5.37
0.6			0.896	0.860	0.865			1.03	1.41	2.21
0.7			0.893	0.806	0.763			0.900	0.951	1.13
0.8			0.930	0.832	0.750			0.862	0.792	0.776
0.9			0.990	0.931	0.852			0.872	0.775	0.707
1.0			1.050	1.060	1.051			0.900	0.806	0.748
1.2			1.130	1.263	1.391			0.953	0.911	0.878
1.4			1.158	1.350	1.543			0.984	0.971	0.894
1.6			1.159	1.354	1.584			0.999	0.999	1.000
1.8			1.148	1.332	1.530			1.006	1.012	1.025
2.0			1.133	1.299	1.476			1.009	1.017	1.023
3.0			1.073	1.162	1.260			1.009	1.015	1.020
4.0			1.045	1.108	1.148			1.006	1.010	1.013
5.0				1.067	1.095			1.004	1.007	1.009
6.0				1.042	1.070			1.003	1.005	1.000
7.0					1.048					
8.0					1.031					

DAA$_2^{(C)}$ ERROR IS OVER FIVE PERCENT IN RANGES:

n=2	$1.2 < \omega < 12.0$	Im Z_n (REACTANCE)	$\omega < 1.4$	Re Z_n (RESISTANCE)
n=3	$1.6 < \omega < 24.0$		$\omega < 1.4$	
n=4	$2.5 < \omega < 35.0$		$\omega < 1.6$	

TABLE 2 · CONVERGENCE OF DAA$_2^{(C)}$/ MODAL ACOUSTIC REACTANCE FOR VARIOUS SPHERICAL SURFACE GRIDS

RATIOS OF Im Z_n: (DAA$_2^{(C)}$/EXACT MODAL SERIES)

$\frac{\omega}{n+1}$	I=24	I=96	I=216	I=384	I=600	EXACT DAA$_2^{(C)}$	I=216	I=384	I=600	EXACT DAA$_2^{(C)}$
		n=1	MODE					n=3	MODE	
0.1	0.869	0.944	0.969	0.989	0.994	1.000	0.988	0.984	0.993	1.006
0.2	0.857	0.960	0.981	0.988	0.993		0.976	0.994	1.004	1.017
0.3	0.848	0.958	0.980	0.988	0.993		0.979	0.999	1.009	1.023
0.4	0.854	0.962	0.983	0.989	0.993		0.958	0.979	0.989	1.004
0.5	0.885	0.975	0.989	0.993	0.996					
0.6	0.942	0.993	0.998	0.999	0.999					
0.7	1.014	1.013	1.007	1.004	1.003					
0.8	1.086	1.029	1.014	1.009	1.005					
0.9	1.142	1.040	1.018	1.011	1.007		(*)			
1.0	1.179	1.045	1.021	1.013	1.008					
1.2	1.203	1.046	1.021	1.013	1.008					
1.4	1.192	1.042	1.019	1.010	1.007					
1.6	1.169	1.036	1.016	1.009	1.006					
1.8	1.146	1.030	1.014	1.007	1.005					
2.0	1.125	1.026	1.012	1.003	1.004					

$\frac{\omega}{n+1}$	I=24		n=2	MODE				n=4	MODE	
0.1		0.947	0.878	0.987	0.994	1.004			0.984	1.005
0.2		0.960	0.983	0.994	1.000	1.012			0.996	1.018
0.3	(*)	0.940	0.977	0.987	0.995	1.007	(*)	(*)	1.006	1.031
0.4		0.931	0.969	0.980	0.988	0.980			0.997	1.023
0.5					—				0.945	0.970

(*) MESH INADEQUATE TO DEFINE FLUID BOUNDARY EIGENVALUES
(*) OUTSIDE RANGE OF DAA$_2^{(C)}$ VALIDITY.

RATIOS OF Re Z_n: (DAA$_2^{(C)}$/EXACT MODAL SERIES)

$\frac{\omega}{n+1}$	I=24	I=96	I=216	I=384	I=600	EXACT DAA$_2^{(C)}$	I=216	I=384	I=600	EXACT DAA$_2^{(C)}$
		n=1	MODE					n=3	MODE	
0.1	0.500	0.750	1.000	1.000	1.000	1.000				
0.2	0.469	0.813	0.906	0.938	0.953					
0.3	0.481	0.828	0.814	0.924	0.966					
0.4	0.487	0.844	0.924	0.952	0.971					
0.5	0.554	0.867	0.937	0.961	0.976					
0.6	0.619	0.897	0.952	0.970	0.982			(*)		
0.7	0.698	0.926	0.966	0.979	0.988					
0.8	0.778	0.952	0.978	0.987	0.992					
0.9	0.850	0.971	0.987	0.992	0.995					
1.0	0.907	0.984	0.993	0.996	0.998					
1.2	0.977	0.998	0.999	1.000	1.000					
1.4	1.007	1.004	1.002	1.001	1.001		0.973	0.973	0.972	0.971
1.6	1.019	1.005	1.002	1.002	1.001		1.003	1.003	1.001	0.999
1.8	1.023	1.006	1.003	1.002	1.001		1.021	1.017	1.015	1.012
2.0	1.023	1.005	1.003	1.002	1.001		1.026	1.022	1.020	1.017

($\le$1.4)		n=2	MODE					n=4	MODE	
1.4		0.988	0.986	0.986	0.985	0.984				
1.6	(*)	1.010	1.004	1.002	1.001	0.999			1.004	1.004
1.8		1.018	1.011	1.009	1.008	1.006	(*)	(*)	1.022	1.005
2.0		1.021	1.014	1.012	1.011	1.009			1.028	1.005
3.0		1.021	1.014	1.012	1.011	1.009				

(*) : MESH INADEQUATE TO DEFINE FLUID BOUNDARY EIGENVALUES.
(*) : OUTSIDE RANGE OF DAA$_2^{(C)}$ VALIDITY.

TABLE 4 · CONVERGENCE OF DAA$_2^{(C)}$ FLUID BOUNDARY EIGENVALUES FOR INCREASING SPHERICAL SURFACE GRID DENSITY

RATIOS OF DAA$_2^{(C)}$ λ_n: (APPROX./EXACT)

n	EXACT λ_n	I=24	I=96	I=216	I=384	I=600
0	1.0	.943	.988	.993	.996	.997
1	.50	.874	.965	.984	990	.994
2	.3333	.796-.88	.946	.976	.985	.991
3	.25	.828-.88	.924-.932	.984	.980	.988
4	.20	.875-1.015	.910-.925	.955	.975	.980

THEORETICALLY DEGENERATE MULTIPLE EIGENVALUES OF LIKE n-ORDER, DIFFERING m-ORDER, NOT RESOLVED FOR n, I COMBINATIONS BELOW SOLID LINE.

TABLE 5 · REQUIRED SWEEPS-STAGS FLUID ELEMENT MESH DENSITIES FOR ACCURATE PREDICTION OF MODAL ACOUSTIC IMPEDANCE

I	ELEMENTS IN CIRCUM. ARC	ELEMENTS PER MODAL HALF WAVE			
		n=1 2 HALFWAVES	n=2 4 HALFWAVES	n=3 6 HALFWAVES	n=4 8 HALFWAVES
24	8	4	2	1.33	1
96	16	8	4	2.67	2
216	24	12	6	4	3
384	32	16	8	5.33	4
600	40	20	10	6.67	5

MESH DENSITIES BELOW THESE LINES RESOLVE THESE VARIABLES TO WITHIN FIVE PERCENT OF EXACT VALUES:

········· FLUID BOUNDARY EIGENVALUES λ_n
– – – – MODAL ACOUSTIC REACTANCE Im Z_n
–·–·– MODAL ACOUSTIC RESISTANCE Re Z_n

were of the same order as the spacing between eigenvalues of adjacent axisymmetric n-orders. All of this data implies minimum required grid densities for acoustic resistance and reactance prediction in frequency ranges of DAA$_2^{(C)}$ validity, as limited by λ_n resolution.

Table 5 summarizes the convergence behavior of n=1, 2, 3 and 4 fluid boundary eigenvalues, acoustic reactances, and acoustic resistances for several different SWEEPS-STAGS fluid element grids. The number of elements per half-wave of the modal pattern required to resolve fluid boundary eigenvalues and modal acoustic impedance functions accurate to five percent depends somewhat on the fluid eigenmode shape. The n=1 mode seems to require special consideration. It is fair to conclude, however, that a minimum of 5 elements per half-wave is needed for five percent accuracy in fluid boundary eigenvalue and resistive fluid impedance prediction in the range $\omega \geq 1.4$ for n=2 and 3 and for $\omega \geq 1.6$ for n=4. Similar requirements seem to hold for minimizing spatial discretization errors in reactive impedance ("added mass" effect) predictions at relatively low frequencies. These tentative mesh requirements in SWEEP-STAGS submerged structure vibration analysis may be substantially altered by inclusion of structural impedance and/or structural damping. Also, convergence of far-field radiation will probably not be as sensitive to grid density as the near-field variables considered in this work.

CONCLUSIONS

This work provides some initial guidelines on required SWEEPS-STAGS fluid grid density needed for accurate representation of acoustic impedance on a surface exposed to exterior fluid. These guidelines should be useful in developing analytical idealizations of complicated submerged structures. The required fluid grid density for five percent error in acoustic impedance is five elements per half-wave in frequency ranges where DAA2 is valid. This requirement is rather demanding and certainly reflects the low interpolation order of fluid variables in the SWEEPS-STAGS fluid elements. Further studies should be undertaken to determine whether the total wet surface input impedance of a submerged structure of interest is governed by structural impedance (mass, stiffness, and structural damping) or by acoustic impedance. It is

7

likely that the surface grid requirements for accuracy of structural vibration prediction would vary according to the topographic details of the structure, the distribution and phasing of the input loads, and the stiffness of local regions of the structure. On the other hand, accurate prediction of far-field radiated sound pressure in the fluid remote from the structure would probably not be as sensitive to surface grid density.

ACKNOWLEDGMENTS

REFERENCES

1 Geers, T. L. and C. A. Felippa, "Doubly Asymptotic Approximations for Vibration Analysis of Submerged Structures," J. Acous. Soc. Am., Vol. 73, No. 4, Apr. 1983, pp. 1152-1159.

2. DeRuntz, J. A. and I. C. Mathews, "A Usage Primer for the Underwater Acoustic Radiation and Scattering Codes SWEEPS and ACRAD," Lockheed Palo Alto Research Laboratory Report LMSC-F035407, Jan 1985.

3 DeRuntz, J. A. and T. L. Geers, "Added Mass Computation by the Boundary Integral Method," Int. J. Num. Meth. Eng., Vol. 12, 1978, pp. 531-549.

4 Zienkiewicz, O. C., The Finite Element Method, Third Edition, McGraw-Hill Book Company (UK) Ltd., London, England, 1977.

5. Zienkiewicz, O. C. and R. E. Newton, "Coupled Vibrations of a Submerged Structure in a Compressible Fluid," ISD-ISSC Proceedings on Finite Element Techniques. Stuttgart, W. Germany, June 1969.

6. Kalinowski, A. J., "Fluid-Structure Interaction Solutions using Finite Elements," Proc. Fifth Navy NASTRAN Colloquium, DTNSRDC Computation and Mathematics Department Technical Memo CMD-32-74. Sept 1974. pp. 71-86.

7. Everstine, G. C., "A Symmetric Potential Formulation for Fluid-Structure Interaction," J. Sound Vibration, Vol 79, No. 1, 1981, pp. 157-160.

8. Wilton, D. T., "Acoustic Radiation and Scattering from Elastic Structures," Int. Journ. Num. Meth. Eng., Vol 13, 1978, pp 123-138.

9 Bronowicki, A. J. and R. B Nelson, "Structural and Acoustic Response of Submerged Axisymmetric Shells," Computational Methods for Infinite Domain Media-Structure Interaction, ASME AMD Vol. 46, 1981. pp. 37-66.

10 Huang, H., "Helmholtz Integral Equations for Fluid-Structure Interaction," Advances in Fluid Structure Interaction — 1984, ASME AMD Vol. 64, ASME, New York, 1984, pp 19-36.

11. Henderson, F. M., "A Structure-Fluid Interaction Capability for the NASA Structural Analysis (NASTRAN) Computer Program," NSRDC Report 3962, Aug 1972.

12 Budzik, E. S., D. T. Pan, L. H Chen, "A Computer Program for Predicting Acoustic Radiation of Finite Elastic Shells with Internal Structure," General Dynamics Electric Boat Division Report U440-74-030, April 1974.

13 Kalinowski, A. J and C. W. Nebelung, "Solution of Axisymmetric Fluid-Structure Interaction Problems with NASTRAN," Tenth NASTRAN User's Colloquium, NASA CP-2249, May 1982, pp 87-111.

14 Everstine, G. C., F. M. Henderson and R. R. Lipman, "Finite Element Prediction of Acoustic Scattering and Radiation from Submerged Elastic Structures," Twelfth NASTRAN User's Colloquium. NASA CP 2328. May 1984, pp 197-209.

15 Mathews, I. C., "A Symmetric Boundary Integral Finite Element Approach for 3-D Fluid Structure Interaction," Advances in Fluid Structure Interaction — 1984, ASME AMD Vol. 64, ASME New York, 1984, pp 39-48.

16. Geers, T. L., "Doubly Asymptotic Approximations for Transient Motions of Submerged Structures," J. Acous. Soc. Am., Vol. 64, No. 5, Nov 1978, pp. 1500-1508.

17 Huang, H and Y. F Wang, "Asymptotic Fluid-Structure Interaction Theories for Acoustic Radiation Prediction," Advances in Fluid-Structure Interaction — 1984, ASME AMD Vol 64, ASME, New York, 1984, pp 1-18.

18. DeRuntz, J. A., "Application of the Underwater Shock Analysis (USA) Code to the Scattering of an Acoustic Signal," Lockheed Palo Alto Research Laboratory report LMSC-D877489, Jan 1983.

19 Geers, T. L., "Transient Response Analysis of Submerged Structures," Finite Element Analysis of Transient Nonlinear Behavior, ASME AMD Vol 14, ASME, New York, 1975, pp 59-84.

20 Felippa, C. A., "Top-Down Derivation of Doubly Asymptotic Approximations for Structure-Fluid Interaction Analysis," Innovative Numerical Analysis for the Applied Engineering Sciences, Proc. Second International Symposium. Univ. Press of Va., 1980, pp. 79-88.

21 Felippa, C. A. and T. L. Geers, "Axisymmetric Free Vibration of a Submerged Spherical Shell," J. Acous. Soc. Am., Vol 67, No 5, May 1980, pp. 1427-1431.

22. DeRuntz, J. A. and F. A. Brogan, "Underwater Shock Analysis of Nonlinear Structures, a Reference Manual for the USA STAGS Code (Version 3)," DNA Report 5545F, Dec 1980.

23. Junger, M. C. and D. Feit, Sound, Structures, and their Interaction, MIT Press, Cambridge, Mass., 1972.

APPENDIX

MODAL IMPEDANCE FUNCTIONS IMPLIED BY DAA2 DIFFERENTIAL EQUATIONS

The DAA2 differential equation relating the wet surface velocity vector $\underline{u}$ to the surface pressure vector $\underline{p}$ is, for coupled modal responses

$$\underline{M}_f \dot{\underline{p}} + \rho c \underline{A}_f \underline{p} + \rho c \underline{Q}_f \underline{A}_f \underline{p} = \rho c (\underline{M}_f \ddot{\underline{u}} + \underline{Q}_f \underline{M}_f \dot{\underline{u}}) \tag{A1}$$

The matrix $\underline{Q}_f$ is an explicit function of wet surface curvature, and is an implicit function of the wet surface's "fluid boundary modes" which are the eigenfunctions of the zero-frequency hydrodynamic eigenproblem:

$$\underline{M}_f \underline{u} = \lambda \underline{A}_f \underline{u} \tag{A2}$$

In "mode-derived" DAA2 (DAA$_2^{(m)}$), $\underline{Q}_f$ is defined by the following, with the curvature parameter "g" restricted to the given range.

$$\underline{Q}_f^{(m)} = g \rho c \underline{A}_f \underline{M}_f^{-1}, \; 0 < g < 1.0 \tag{A3}$$

In "curvature-augmented" DAA2 (DAA$_2^{(c)}$), $\underline{Q}_f$ is defined in terms of a matrix of local wet surface curvatures $\underline{K}$

$$\underline{Q}_f^{(c)} = \rho c \underline{A}_f \underline{M}_f^{-1} - c\underline{K} \tag{A4}$$

In DAA$_2^{(m)}$, the parameter g is, heuristically, a measure of the average curvature of acoustic waves emitted by the radiating wet surface. The lower bound value $g=0$ reduces second-order DAA$_2^{(m)}$ to first-order DAA1, in which the limiting high frequency fluid impedance asymptote is ρc, the impedance exhibited by plane waves. The other extreme, $g=1.0$, has produced reasonable results in a USA-STAGS spherical shell scattering problem [18], while $g=0.5$ was found appropriate in transient response prediction of a shock wave-excited infinitely long cylindrical shell [22]. These two values of g are appropriate to spherical and cylindrical wave curvature.

respectively, since these are the dominant acoustic waveforms near the wet surface of these two idealized structural boundaries.

The level of acoustic discretization (fluid boundary element density) is an issue impacting the performance of both DAA2 forms. In DAA$_2^{(m)}$, the curvature parameter g is an additional consideration that is handled rationally in DAA$_2^{(c)}$. The ability of DAA2 acoustic fluid models to represent the fluid boundary eigenmodes of some simple radiating surface geometries is of interest here. The above two DAA2 versions can be written in uncoupled mode form. these equations will be used to derive implied corresponding specific acoustic impedance functions. for which exact solutions exist for acoustically uncoupled geometries. The modal DAA2 equations are specializations of equations (A1) and (A2).

$$\text{DAA}_2^{(m)} \quad m_n p + \rho c a_n p + \rho c \omega_n^{(m)} a_n p =$$
$$\rho c (m_n u + \omega_n^{(m)} m_n u), \quad \omega_n^{(m)} = g \rho \left(\frac{a_n}{m_n} \right) \tag{A5}$$

$$\text{DAA}_2^{(c)} \quad \text{(A5) above. with } \omega_n^{(c)} = \rho c \left(\frac{a_n}{m_n} \right) - c K_n \tag{A6}$$

substituted for $\omega_n^{(m)}$

Geers has shown [16] that g is related to fluid boundary eigenvalues. If λ_n are the eigenvalues of

$$m_n u_n = \lambda_n a_n u_n. \tag{A7}$$

then the mode-derived $\omega_n^{(m)} \sigma_n$ must be restricted to the range

$$0 \leq \omega_n^{(m)} \leq \sigma_n. \tag{A8}$$

where

$$\sigma_n = \rho c \lambda_n \tag{A9}$$

These considerations. given that $\lambda_n = m_n / a_n$, establish the terms $\omega_n^{(m)}$ as shown in equation (A5).

The specific acoustic impedances implied by equations (A5) and (A6) for radiator surfaces demonstrating uncoupled modes can be derived by applying Laplace transforms to (A5) and (A6). The results are

$$\text{DAA}_2^{(m)} \quad (m_n s^2 + \rho c a_n s + \rho c \omega_n^{(m)} a_n) p =$$
$$(\rho c m_n s^2 + \rho c \omega_n^{(m)} m_n s) u \tag{A10}$$

$$\text{DAA}_2^{(c)} \quad \text{(A10) above. with } \omega_n^{(c)} \text{ replacing } \omega_n^{(m)} \tag{A11}$$

If velocity u is taken to be modal velocity u_n then equations (A10) and (A11) can be used to define complex-valued modal impedances

$$Z_n \text{ DAA}_2^{(m)} = \frac{p}{u_n} = \frac{\rho c (m_n s^2 + \omega_n^{(m)} m_n s)}{m_n s^2 + \rho c a_n s + \rho c \omega_n^{(m)} a_n} \tag{A12}$$

$$Z_n \text{ DAA}_2^{(c)} \quad \text{(A12) above with } \omega_n^{(c)} \text{ replacing } \omega_n^{(m)} \tag{A13}$$

Since the transform variable s becomes $j\omega$ for harmonic time-dependence of all variables. equations (A12) and (A13) become. after some algebra and use of some new variables

$$m_n a_n = \lambda_n$$

$$\Omega_n^{(c)} = \rho - K_n \lambda_n$$

$$Z_n \text{ DAA}_2^{(m)} = \rho c \left[\frac{\rho c \lambda_n j\omega - \lambda_n^2 \omega^2}{\rho c^2 g + \rho c \lambda_n j\omega - \lambda_n^2 \omega^2} \right] \tag{A14}$$

$$Z_n \text{ DAA}_2^{(c)} = \rho c \left[\frac{c \Omega_n \lambda_n j\omega - \lambda_n^2 \omega^2}{\rho c^2 \Omega_n + \rho c \lambda_n j\omega - \lambda_n^2 \omega^2} \right] \tag{A15}$$

After further complex arithmetic. and separation into real and imaginary parts. the following modal impedance functions particular to the two DAA2 forms are obtained

$$\text{Re} Z_n \text{ DAA}_2^{(m)} = \rho c \left[\frac{\omega^4}{\left(\omega^2 - g \left(\frac{\rho c}{\lambda_n} \right)^2 \right)^2 + \left(\frac{\rho c}{\lambda_n} \right)^2 \omega^2} \right]$$

$$\frac{\text{Im} Z_n \text{ DAA}_2^{(m)}}{j\omega} = \rho c \left[\frac{\left(\frac{\rho c}{\lambda_n} \right)^3 g^2 + \left(\frac{\rho c}{\lambda_n} \right)(1 - g)\omega^2}{\left(\omega^2 - g \left(\frac{\rho c}{\lambda_n} \right)^2 \right)^2 + \left(\frac{\rho c}{\lambda_n} \right)^2 \omega^2} \right] \tag{A16}$$

$$\text{Re} Z_n \text{ DAA}_2^{(c)} = \rho c \left[\frac{\omega^4}{\left(\omega^2 - \frac{\Omega_n}{\rho} \left(\frac{\rho c}{\lambda_n} \right)^2 \right)^2 + \left(\frac{\rho c}{\lambda_n} \right)^2 \omega^2} \right]$$

$$\frac{\text{Im} Z_n \text{ DAA}_2^{(c)}}{j\omega} = \rho c \left[\frac{\left(\frac{\rho c}{\lambda_n} \right)^3 \left(\frac{\Omega_n}{\rho} \right)^2 + \left(\frac{\rho c}{\lambda_n} \right)\left(1 - \frac{\Omega_n}{\rho} \right)\omega^2}{\left(\omega^2 - \frac{\Omega_n}{\rho} \left(\frac{\rho c}{\lambda_n} \right)^2 \right)^2 + \left(\frac{\rho c}{\lambda_n} \right)^2 \omega^2} \right] \tag{A17}$$

where $\lambda_n = m_n / a_n$ and $\Omega_n = (\rho - K_n \lambda_n)$

These expressions depend on fluid boundary eigenvalues λ_n. which are equivalent to modal accessions to inertia per unit radiating surface area m_n / a_n. and the radiated-wave curvature parameters g (DAA$_2^{(m)}$) or K_n (DAA$_2^{(c)}$). It should be pointed out that fluid boundary eigenvalues correspond to low frequency asymptotic limits of "accession to inertia per unit area". Exact expressions of modal accessions to inertia for the sphere and the infinite cylinder are given in Junger and Feit [23]. who also present low frequency asymptotic expressions. For axisymmetric modes the low frequency limit of λ_n for a spherical surface is

$$\lambda_n \text{ (sphere)} = \frac{\rho r}{n+1} \quad (kr)^2 \ll 2n-1 \tag{8.31 ref 23}$$

9